

# Cooperative enhancement of two-photon absorption in self-assembled zinc-porphyrin nanostructures

Alexander Mikhaylov,<sup>a</sup> Dmitry V. Kondratiuk,<sup>b</sup> Arjen Cnossen,<sup>b</sup> Harry L. Anderson,<sup>b\*</sup> Mikhail Drobizhev,<sup>a</sup> and Aleksander Rebane<sup>a,c\*</sup>

<sup>a</sup> Department of Physics, Montana State University, Bozeman, MT 59717, USA.

<sup>b</sup> Oxford University, Department of Chemistry, Oxford, OX1 3TA, UK.

<sup>c</sup> National Institute of Chemical Physics and Biophysics, Tallinn 12618, Estonia

## Abstract.

Femtosecond two-photon absorption (2PA) spectra were measured of a series of butadiyne-linked zinc-porphyrin oligomers assembled in single- and double-strand linear and cyclic structures containing 6, 12 or 24 porphyrin units, in the excitation wavelength range 900–1600 nm. We observe strong enhancement of the 2PA cross-section in the Soret region, with maximum values up to  $\sigma_{2PA} \sim 10^5$  GM depending on the geometry of the construct, which we quantitatively explain in terms of a three essential energy level model and cooperative enhancement of the transition dipole moments between the states. The Zn-coordinated template-bound ring of 6 porphyrin units, which resembles some natural light-harvesting systems, results in the highest 2PA cross-section per porphyrin unit ( $\sim 10^4$  GM). It is remarkable that this molecule gives such strong  $\sigma_{2PA}$ , when the  $S_0$ - $S_1$  (0-0) transition is essentially forbidden.

## Introduction

Porphyrins and their derivatives possess a diverse collection of intriguing chemical and physical properties that are extensively exploited by nature. Light-harvesting in photosynthesis is accomplished by special chlorophyll complexes, often involving chromophore units arranged in ring- or cylinder-like structures to maximize the energy capture and transfer efficiency<sup>1,2</sup>. The last decades have witnessed a broad range of spectroscopic investigations of excitation and relaxation dynamic properties of chromophores involved in photosynthesis, including some man-made porphyrin-based assemblies designed to implement the light-harvesting function<sup>3,4</sup>. However, to achieve the long-standing goals of efficient artificial photosynthesis, further studies are warranted to gain more detailed quantitative understanding of the creation and evolution of delocalized electronic excitations and their dependence on the mutual spatial arrangement of the chromophores.

Measurements and theoretical calculations of the instantaneous two-photon absorption (2PA) cross section,  $\sigma_{2PA}$ , and its wavelength dependence was recently used to study and quantify the extent of conjugation in porphyrin dimers<sup>5-7</sup>, linear porphyrin oligomers<sup>8-11</sup>, in conjugated dendrimers<sup>12-15</sup>, cyclic thiophenes<sup>16</sup> and expanded porphyrins<sup>17</sup>. A cooperative enhancement effect is observed when the maximum 2PA cross section, calculated per porphyrin or other elementary chromophore building block, is considerably larger for the complex compared to that of an individual unit<sup>18</sup>. The idea behind this approach is based on the fact that the peak value of  $\sigma_{2PA}$  corresponding to a certain 2PA transition to higher-energy states, increases in proportion to the value of transition dipole moments between the ground and excited states and between the excited states, which in turn depends on how many building blocks or chromophore units are coherently interacting ( $\pi$ -conjugated)<sup>5,19</sup>. Linear porphyrin oligomers containing up to about 13

Zn-porphyrin units showed a dramatic up to 10–500 times enhancement of the peak 2PA cross-sections (per porphyrin unit) compared to the monomers<sup>8,9</sup>, from which average conjugation length encompassing 4–6 units depending on the planarity of the chain was estimated.

Here we apply two-photon spectroscopy to elucidate the conjugation in butadiyne-linked zinc-porphyrin oligomers arranged in a variety of different geometries comprising single- and double-strand linear, conjugated nanorings, as well as a “figure-of-eight” type 12-mer and a template-bound hexamer nanoring. We measure the femtosecond 2PA cross sections in the excitation wavelength range 900–1600 nm that includes a strongly 2-photon allowed transition and determine the corresponding maximum  $\sigma_{2PA}$  values, which allows us to estimate the cooperative enhancement factor.

## Experimental Section

**Figs. 1** illustrates the molecular structures of the eight compounds studied in this work. ***l*-P6** and ***l*-P12** (**Fig. 1a**) represent 6- and 12-unit linear oligomers connected at opposing *meso*-positions via butadiyne linker groups. ***c*-P12** is a cyclic oligomer comprising 12 units of Zn-porphyrins (**Fig. 1b**). Adding a small amount of bidentate Zn-coordinating agent **DABCO** to the toluene solution of ***l*-P12** or ***c*-P12** causes self-assembly of a double-strand ladder (***l*-P12**)<sub>2</sub>•(**DABCO**)<sub>12</sub> (**Fig. 1c**) or sandwich (***c*-P12**)<sub>2</sub>•(**DABCO**)<sub>12</sub> (**Fig. 1d and e**), respectively. ***c*-P6•T6** is another cyclic oligomer comprising 6 *meso*-linked Zn-porphyrins, which are coordinated to a core template (**Fig. 1f**). ***c*-P12•(T6)**<sub>2</sub> contains a 12-unit cyclic oligomer that is attached simultaneously to two templates in a figure-of-eight structure (**Fig. 1g**).

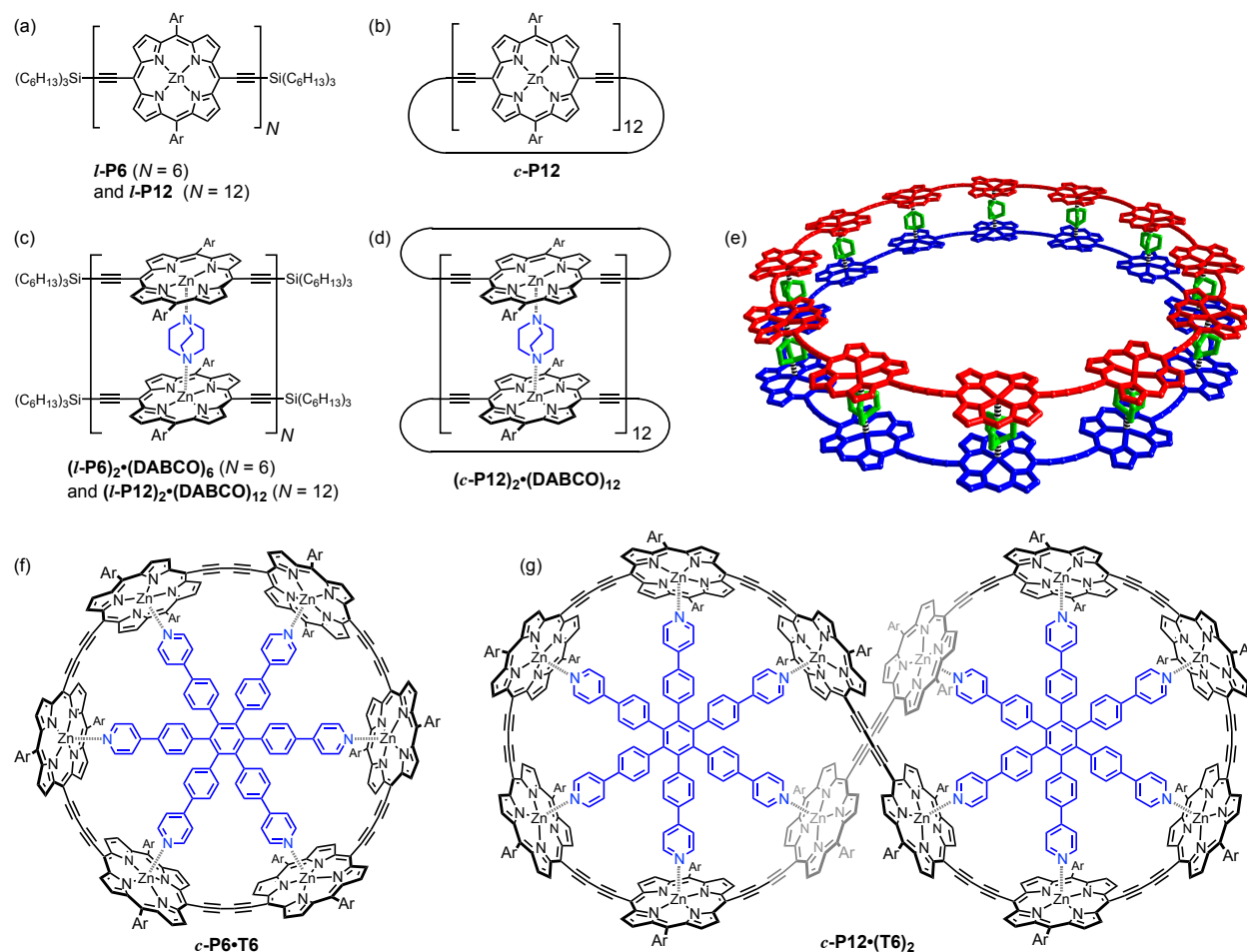


**Figure 1.** Structures of the supramolecular porphyrin systems under study: (a) linear oligomers  $l\text{-P6}$  and  $l\text{-P12}$ ; (b) cyclic nanoring  $c\text{-P12}$ ; (c) linear double-strand ladder complexes  $(l\text{-P6})_2 \cdot (\text{DABCO})_6$  and  $(l\text{-P12})_2 \cdot (\text{DABCO})_{12}$ ; (d) and (e) double-strand sandwich complex  $(c\text{-P12})_2 \cdot (\text{DABCO})_{12}$ ; (f) cyclic hexamer template complex  $c\text{-P6} \cdot \text{T6}$ ; (g) figure-of-eight complex  $c\text{-P12} \cdot (\text{T6})_2$ . The **DABCO** and **T6** template units are shown in blue. Ar is a 3,5-bis(*n*-octyloxy)phenyl sidechain in all cases except for  $c\text{-P6} \cdot \text{T6}$  in which case the version with 3,5-bis(trihexylsilyl)phenyl sidechains was used for enhanced solubility during nonlinear transmission measurements.

Details of the synthesis were described previously<sup>20-24</sup>. X-ray crystallography, small-angle X-ray scattering, <sup>1</sup>H NMR spectroscopy and scanning tunneling microscopy experiments were used to prove the molecular structures<sup>20-24</sup>.

Spectroscopic samples were prepared in 2 mL of toluene, except for **c-P6-T6**, in which case CCl<sub>4</sub> was used. Samples were contained in 1-cm or 1-mm path length quartz cuvettes (depending on the 2PA measurements method) both for 1PA and 2PA measurements. To avoid aggregation of **c-P12**, **l-P12** and **l-P6**, a small amount of pyridine (~1% by volume of solvent) was added to the toluene solution. To create the double-strand “sandwich” (**c-P12**)<sub>2</sub>·(**DABCO**)<sub>12</sub> and “ladder” (**l-P12**)<sub>2</sub>·(**DABCO**)<sub>12</sub> and (**l-P6**)<sub>2</sub>·(**DABCO**)<sub>6</sub> complexes, a 1 mM solution of **DABCO** in toluene was added to the cuvette to give a **DABCO** concentration of ca. 10–20 μM (mole ratio: 10–20 **DABCO** molecules per porphyrin oligomer). UV-vis-NIR absorption measurements and denaturation titrations (see Supporting Information) confirmed the formation of double-strand complexes. Linear absorption measurements were performed with a PerkinElmer UV/VIS/NIR Lambda 950 spectrometer. For relative quantum yield measurements a luminescence PerkinElmer LS 50B spectrophotometer was used. The sample concentrations used in two-photon excited fluorescence (2PEF) measurements were ~1 μM, while for the nonlinear transmission (NLT) measurement higher concentration ~0.4 mM was required. Optical densities of the samples were measured before and after the 2PEF and NLT measurements. Even though most of the samples were stable under exposure to the laser irradiation, some minor bleaching was observed for (**l-P12**)<sub>2</sub>·(**DABCO**)<sub>12</sub>, which resulted in decrease of the peak optical density by 10–15%.

The 2PEF method was employed to measure the relative 2PA spectra. A Ti:Sapphire femtosecond laser system (Coherent, Libra) operated at 1 kHz repetition rate and produced pulses with duration ~100 fs pumped an optical parametric amplifier (OPA) (Light Conversion, OPerA Solo). The OPA output wavelength was tuned in a region of 900–1600 nm with 2 nm step. The approximate OPA pulse spectral width was ~ 15–35 nm. For detection of the

fluorescent signal, a grating spectrometer (Jobin-Yvon, Triax 550) combined with a CCD detector (Spectrum One) was used. Styryl 9M diluted in  $\text{CHCl}_3$  was used as the reference standard for the 2PEF measurements (for details see ref. 25). The fluorescence quantum yield of **c-P6-T6** is too low for reliable 2PEF measurement<sup>9,24</sup>, and thus femtosecond NLT method was used to determine the 2PA cross sections (for details of the method see ref. 26). Briefly, for the NLT measurement, the same laser setup was employed, but the pulse repetition rate was reduced to 100 Hz. The OPA beam was additionally collimated using a series of apertures and lenses. To detect the change in the transmission, two sets of 10 mm aperture detectors were used: silicon photodetectors (Thorlabs, DET 100A) for the range 900–1120 nm (second harmonic of idler, SHI) nm and InGaAs photodetectors (Thorlabs, DET 20C) for the range 1120–1600 nm (signal). LDS 798 (concentration  $\sim 1$  mM) diluted in  $d_6$  acetone was used as the reference standard for the NLT measurements. In the idler range 1600 – 1950 nm only relative NLT measurements, i.e. without reference standard calibration, were performed using pyroelectric detectors (Molelectron P4-45).

## Results and discussion

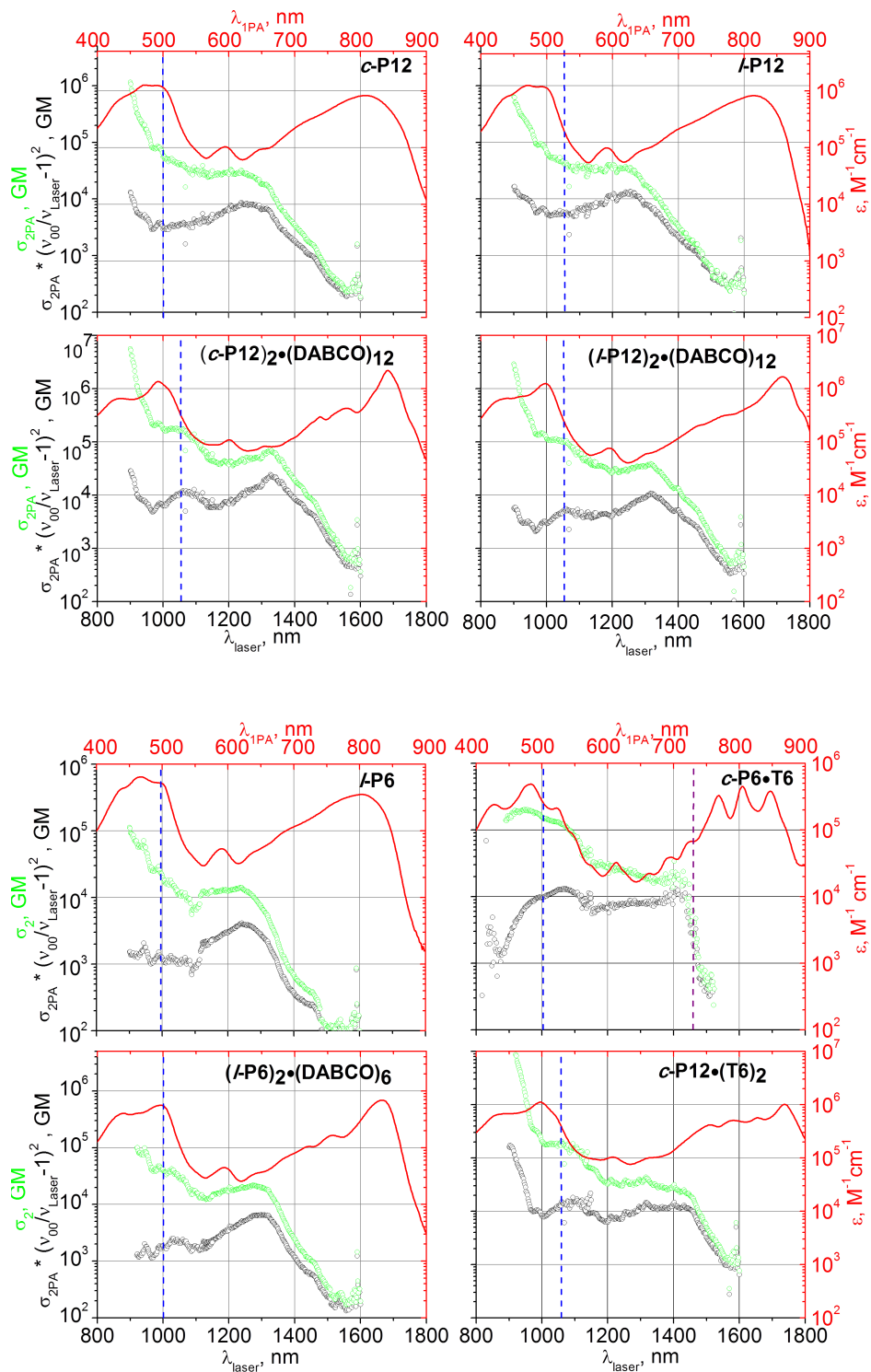




**Figure 2.** 1PA (red line) and 2PA (green dots) spectra of the porphyrin complexes studied. The lower horizontal scale corresponds to the 2PA laser wavelength, while the upper scale represents 1PA wavelength. Values of 2PA cross-section,  $\sigma_{2PA}$ , and the extinction coefficient,  $\epsilon$ , are given per covalent chain. Black symbols represent effective 2PA with the resonance enhancement contribution subtracted (see text for details). Vertical blue dashed line indicates cut-off wavelengths for the quadratic power dependence of the 2PA (see the text for details). All left and all right axes are scaled identically.

The measured 2PA cross section spectra (green symbols) along with the corresponding linear extinction spectra (red curves) are shown in **Fig 2**. The estimated accuracy of the 2PA cross section values is 35%.

All values are presented per covalently bonded cyclic or linear porphyrin chain/ring (self-assembled “sandwich” and “ladder” structure contain two equivalent rings or chains respectively). The 1PA spectra show the Soret bands (400–550 nm) and the Q bands (700–850 nm). In the intermediate region, around  $600 \pm 15$  nm, there is a distinct one-photon transition that can be assigned to  $Q_y$ -band (see Supplementary Information and ref. 10 for details). It was shown that in the dimer the weak peak at around 600 nm is not purely y-polarized<sup>10</sup>. Compared to the single-strand oligomers, the self-assembled double-strand structures show a distinct red shift ( $\sim 1,000 \text{ cm}^{-1}$ ) of the Q-band as well as narrowing of the main features of the 1PA spectra. The narrowest spectral features are observed in the template-bound ring, **c-P6-T6**.

Every effort was made to minimize potential artifacts in determining  $\sigma_{2PA}$ . For the 2PEF method, the quadratic dependence of the detected fluorescence signal on the incident power was verified at selected wavelengths in the range 1000–1600 nm with accuracy,  $2.00 \pm 0.05$ , as illustrated in **Fig. 3**. For the NLT method, the square law characteristic was measured at each wavelength and

was found to be quadratic in the range 1000–1480 nm. **Table 1** shows the 2PEF power exponent values determined throughout the 2PA spectrum at selected wavelengths. At wavelengths shorter than the cut-off wavelength, vertical blue dashed line in **Fig. 2** (and at wavelengths longer than marked with the dashed purple vertical line for **c-P6-T6** as well), the quadratic power exponent starts to decline, most likely due to accompanying 1PA that occurs due to increasing overlap between the laser spectrum and the red wing of the Q-band. 2PA cross sections reach maximum values of  $\sigma_{2PA} \sim 10^5$  GM (per covalently bonded oligomer) in the Soret region (1000–1100 nm), and are presented in **Table 2**. The 2PA cross section drops rapidly by several orders of magnitude towards the Q-band ( $\lambda > 1400$  nm), which is characteristic of porphyrin systems lacking strong electron-accepting or donating substituents. In the intermediate region, around 1250–1400 nm, the 2PA cross section has values in the range  $\sim 10^3$ – $10^5$  GM. The 2PA spectra of the unbound oligomers provide a hint of a transition peak in the range,  $\lambda_{laser} = 1250$ – $1350$  nm, which is distinctly different from all features including the 600 nm peak observed in the 1PA spectrum. The template-bound oligomers show a slightly different behavior, where a broad peak is observed at longer wavelengths around 1400 nm, which may in part overlap with the vibronic progression associated with Q-region.

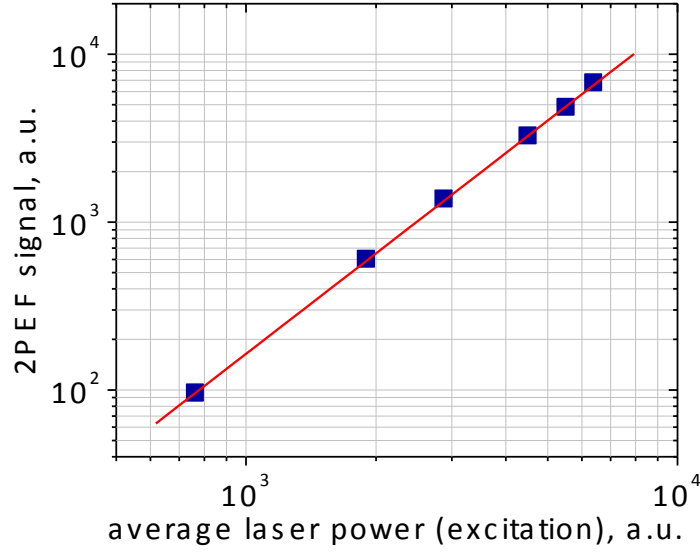


**Figure 3.** Quadratic dependence of the 2PEF signal on the average laser (excitation) power for  $(l\text{-P6})_2\bullet(\text{DABCO})_6$  plotted in the double logarithmic scale (symbols) at  $\lambda_{\text{laser}} = 1000$  nm. The data are fitted with a linear function with the slope  $B = 1.99 \pm 0.01$  (red line)

**Table 1.** Quadratic power dependence for the 2PEF measurements. The exponents are close to 2 for all samples. The excitation wavelengths are presented in the parentheses.

Sample	Exponents from fitting
<i>c</i> -P12	1.98 (1000 nm)
$(c\text{-P12})_2\bullet(\text{DABCO})_{12}$	1.95 (1050 nm)
<i>l</i> -P12	1.95 (1050 nm)
$(l\text{-P12})_2\bullet(\text{DABCO})_{12}$	1.95 (1050 nm)
<i>l</i> -P6	1.99 (1000 nm)
$(l\text{-P6})_2\bullet(\text{DABCO})_6$	1.99 (1000 nm)
<i>c</i> -P12•(T6) <sub>2</sub>	1.95 (1065 nm)

Even if the quadratic power law is strictly fulfilled, the measured value of  $\sigma_{2PA}$  is still in many instances affected by resonance enhancement effect, which modifies the 2PA spectral shapes at higher energies, depending on the location and strength of the Q-band<sup>5,9</sup>. The resonance factor  $R$  may be expressed as:

$$R(\nu_{laser}) = \left( \frac{\nu_{i0}}{\nu_{laser}} - 1 \right)^2, \quad (1)$$

where  $\nu_{i0}$  is the frequency of Q-band and  $\nu_{laser}$  is the laser frequency. One can account for the effect of resonance enhancement on the measured 2PA spectra by introducing a modified 2-photon cross section  $\sigma_{2PA}'$ <sup>18</sup>:

$$\sigma_{2PA}' = \sigma_{2PA} R(\nu_{laser}). \quad (2)$$

Black symbols in **Fig. 2** show the  $\sigma_{2PA}'$  spectra; the corresponding peak values of  $\sigma_{2PA}'$  are collected in **Table 2**. Recasting the data in terms of  $\sigma_{2PA}'$  increases the prominence of the strongly 2-photon allowed transition at around 1250–1300 nm. This corresponds to transition energy that is about 1.3 times larger than the energy of the Q-transition ( $S_0 \rightarrow S_1$ ), which allows it to be tentatively assigned to the  $A_g \rightarrow mA_g$  transition<sup>8,27,28</sup>.

In the case of the template-bound cyclic oligomer **c-P6-T6**, previous studies including quantum chemical calculations indicate that both the ground and the first electronic excited state belong to the  $A_g$  symmetry, thus rendering the lowest-energy pure electronic transition (corresponding to the 0-0 component of Q-band in 1PA spectrum of regular porphyrins) 1-photon forbidden<sup>20,29</sup>. At the same time, higher vibronic components in the 1PA spectrum (between 750 and 850 nm, **Fig. 2**) are allowed due to Herzberg-Teller intensity borrowing mechanism<sup>20,30,31</sup>. The fact that the

shape of the 2PA spectra of **c-P6-T6** and **c-P12-(T6)<sub>2</sub>** in the intermediate region (**Fig. 2**) is different from the template-free oligomers, may be viewed as an indirect confirmation of these earlier conclusions, and allows us to interpret the 2PA peak near  $\lambda_{\text{laser}} = 1400$  nm as corresponding to another  $A_g \rightarrow A_g$  transition.

A simplified exciton model was employed to explain some main features of  $\pi$ -conjugated porphyrin ring structures, such as one-photon selection rules<sup>30</sup>, however, a more quantitative description should also address the issue of exciton localization<sup>30,31,32</sup>.

The cooperative effect has been found earlier for different types of porphyrin constructs<sup>5,19</sup>. One way to analyze the cooperative enhancement is to scale the measured peak  $\sigma_{2PA}$  with respect to that in the constituent chromophore, which in our case is the porphyrin dimer.<sup>8</sup> The corresponding parameter may be defined for an N-porphyrin unit oligomer as:

$$\xi = \sigma_{2PA}^{\max} / \sigma_{2PA}^{\max}(\text{dimer}) \cdot (2 / N), \quad (3)$$

where  $\sigma_{2PA}^{\max}$  and  $\sigma_{2PA}^{\max}(\text{dimer})$  are, respectively, the maximum 2PA cross-sections for the oligomer under study and of the dimer. The corresponding values are presented in **Table 2**. Perhaps a more quantitative comparison could be carried out if we directly employ the three-level model that was found to provide a reasonable quantitative description of the 2PA properties of a variety of conjugated chromophores including linear porphyrin oligomers of different lengths<sup>8,9,12,33</sup>. According to this model, the peak 2PA cross section of a 2-photon allowed transition may be expressed as (eq. 7a in ref.9):

$$\sigma_{2PA}^{\max} = \frac{(2\pi f)^4}{5(nch)^2} \sqrt{\frac{\ln 2}{\pi}} \frac{|\mathbf{\mu}_{0i}|^2 |\mathbf{\mu}_{if}|^2}{\left(\frac{\nu_{0i}}{\nu_{0f}} - \frac{1}{2}\right)^2 \Gamma}, \quad (4)$$

where  $\mu_{0i}$  and  $\mu_{if}$  are, respectively, the transition dipole moment between ground state,  $0$ , and intermediate state,  $i$ , (in esu units), and the transition dipole moment between intermediate state and the final excited state,  $f$ ,  $n$  is the index of refraction,  $c$  is the speed of light;  $\nu_{0f}$  is the transition frequency between  $0$  and  $f$ , and  $\Gamma$  is the spectral width (FWHM) of the final state (in Hz), and  $f$  is the local optical field enhancement factor:

$$f = \frac{n^2 + 2}{3}. \quad (5)$$

It is also assumed that the transition dipole moment vectors are aligned parallel.

The ground state transition dipole moment is found by integrating the linear absorption spectrum over the Q-band<sup>34</sup>:

$$\mu_{0i}^2 = \frac{3 \times 10^3 \ln 10 \, n \, h \, c}{8\pi^3 f^2 N_A} \int \frac{\varepsilon(\lambda) d\lambda}{\lambda}, \quad (6)$$

where  $N_A$  is the Avogadro number. Substituting  $|\mu_{0i}|^2$  into Eq. (4), we obtained the excited state transition dipole moment values,  $|\mu_{if}|$ , which are given in **Table 2**. The excited state transition dipole moments are comparable in value to the ground state transition dipole moments,  $\mu_{0i}$ , and vary in the range 7.0–20 D, which corresponds to strongly allowed dipole transition, lending support to the idea that the 2PA transition takes place between  $A_g$  and  $mA_g$  of the strongly delocalized states<sup>9,27</sup>.

**Table 2.** 1PA and 2PA parameters for the measured porphyrin complexes.  $N$  is the number of Zn-porphyrins. Final state line width,  $\Gamma$ , was obtained from Gaussian fitting of the lowest energy 2PA peak in the modified  $\sigma_{2PA}'$  spectrum. The values  $\mu_{0i}$ ,  $\mu_{if}$ ,  $\sigma_{2PA}^{\max}$ , and  $\sigma_{2PA}'$  are shown per covalently bound oligomer chain. The values  $\sigma_{2PA}^{\max}$  are presented at the short wavelength maxima in 2PA spectra (wavelengths are shown in parentheses); parameter  $\xi$  shows the effect of the enhancement of 2PA cross section of the porphyrin oligomers with respect to the porphyrin dimer that was measured earlier<sup>8</sup> (see text for details); the values  $\sigma_{2PA}'$  are shown for the lowest energy peak in modified 2PA spectra (see **Eq. 1** and **Fig. 2**).

\* Approximate value average over the vibronic progression.

Sample	$N$	$\nu_{0i}$ $\text{cm}^{-1}$	$\nu_{if}$ $\text{cm}^{-1}$	$\sigma_{2PA}^{\max}$ $10^3 \text{ GM (nm)}$	$\xi$	$\sigma_{2PA}'$ $10^3 \text{ GM}$	$\Gamma$ $\text{cm}^{-1}$	$\mu_{0i}$ D	$\mu_{if}$ D	$S$ $10^5 \text{ GM/cm}$
<b>c-P12</b>	12	12376	16474	65 (1000)	1.4	8.1	1340	28	18	10
<b>(c-P12)<sub>2</sub>•(DABCO)<sub>12</sub></b>	24	11882	15130	170 (1050)	1.9	23	1010	19	42	20
<b>l-P12</b>	12	12853	16615	42 (1050)	0.9	12	1300	29	15	15
<b>(l-P12)<sub>2</sub>•(DABCO)<sub>12</sub></b>	24	11655	15174	106 (1050)	1.2	11	1270	22	30	10
<b>l-P6</b>	6	12468	16233	23 (1000)	1	3.9	1200	19	16	8
<b>(l-P6)<sub>2</sub>•(DABCO)<sub>6</sub></b>	12	12004	15625	38 (1000)	0.8	6.6	1130	15	25	14
<b>c-P12•(T6)<sub>2</sub></b>	12	12088*	15700	173 (1050)	3.8	18	1390	30	30	18
<b>c-P6•T6</b>	6	12350*	16200	151 (1000)	6.6	11	1690	18	50	28

Assuming full  $\pi$ -conjugation for the linear complexes containing  $N$  Zn-porphyrins, the value of the product  $|\mu_{0i}^2| |\mu_{if}^2|$  should scale as,  $\sim N^4$ . In the case of cyclic oligomers, this simple scaling behavior may be strictly speaking not applicable, but in the first approximation we will use the same approach. To quantify the relative scaling of the dipole moments, and to monitor the extent of conjugation, we introduce the following so-called cooperativity factor or conjugation signature<sup>8</sup> defined as:

$$S = \sigma'_{2PA} \Gamma_f N^{-1} \quad (7)$$

The  $S$  values are collected in **Table 2**. The  $S$  value for the linear hexamer **(l-P6)<sub>2</sub>•(DABCO)<sub>6</sub>** correlates very well with the results from the previous study of similar linear porphyrin

oligomers; although the result for the  $(\textbf{I-P12})_2\cdot(\textbf{DABCO})_{12}$  slightly deviates from the general trend observed earlier<sup>8</sup>. Forming the double-strand hexamer “ladder” complex increases the  $S$  value by almost a factor of 2 compared to the single-strand. At the same time, formation of the double-strand “ladder” of the 12-porphyrin linear oligomer decreases the cooperativity slightly, compared to single-strand, which may indicate some saturation (however, such saturation was not detected earlier for similar systems<sup>8</sup>). For the 12-porphyrin ring, the corresponding increase of  $S$  is a factor of two. Stronger cooperativity may arise because axially oriented orbitals provide a better total overlap, although this effect may also be due to smaller disorder along the ring<sup>18,35</sup>.

The templated 6-unit ring  $\textbf{c-P6}\cdot\textbf{T6}$  stands out because of its markedly higher  $S$  value compared to all the other complexes. It was demonstrated previously that in this system the conjugation embraces the whole ring<sup>20,30,36</sup>, as would be supported by the specific features of the 1PA spectra such as narrow line width and disallowed  $S_0-S_1$  (0-0) transition. The triplet excited state of  $\textbf{c-P6}\cdot\textbf{T6}$  is delocalized over all 6 porphyrin rings, which is remarkable because triplet excited states are normally less delocalized than singlets and the triplet state of the linear oligomers are only delocalized over two porphyrin centers<sup>36</sup>. It appears that the core template may be providing additional rigidity to the molecular structure, resulting in more extensive conjugation<sup>23</sup>. In the case of the “figure-of-eight” complex  $\textbf{c-P12}\cdot(\textbf{T6})_2$ , the conjugation appears to be partially broken, although the X-ray crystal structure of this compound<sup>22</sup> shows that the torsional angles between neighboring porphyrin units are all less than  $20^\circ$ , which should not interrupt the  $\pi$ -overlap.

To gain some additional insight into the nature of the  $S_0-S_1$  (0-0) transition, we measured the NLT spectrum of  $\textbf{c-P6}\cdot\textbf{T6}$  in the idler wavelength range, 1550 – 1950 nm. Unfortunately, due to lack of suitable reference standards, our ability to apply laser correction to the relative spectral



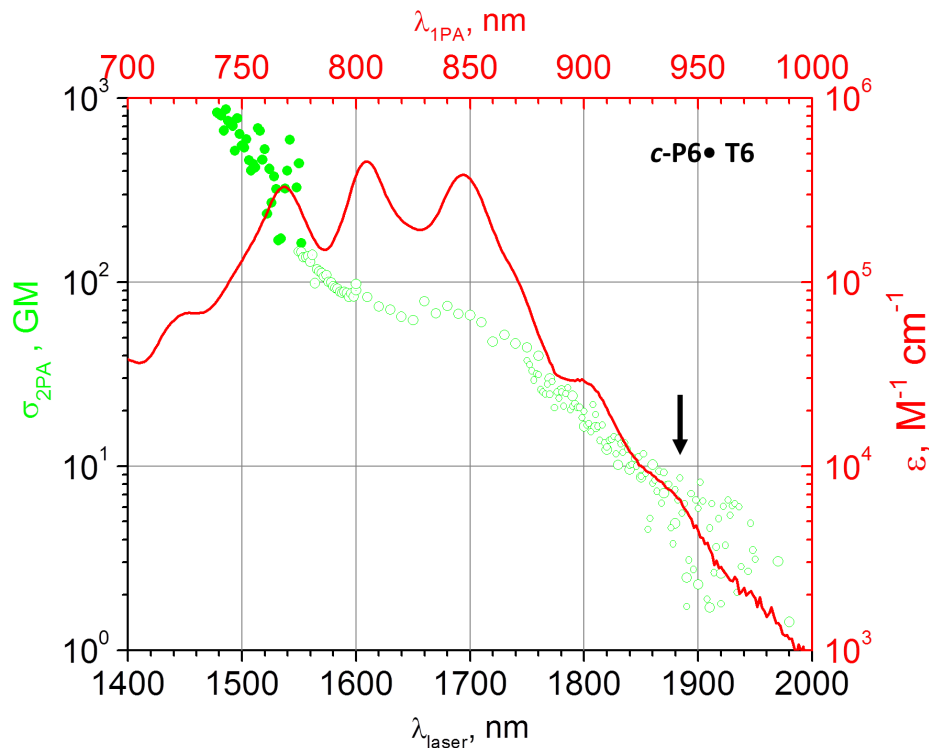


**Figure 4.** 1PA (red line) and 2PA (green symbols) spectra of **c-P6•T6** porphyrin construct. Empty symbols show non-corrected 2PA spectrum scaled to match at 1550 nm to corrected spectrum (filled symbols). The black arrow (at 946 nm) indicates theoretically predicted (0-0) transition<sup>20</sup>. The lower horizontal scale corresponds to the 2PA laser wavelength, while the upper scale represents 1PA wavelength

shape and the 2PA cross section, were limited. **Fig. 4** shows the non-corrected spectrum of **c-P6•T6** in  $\text{CCl}_4$  solution measured in the presumed (0-0) transition region (empty symbols), where the cross section is estimated by matching the values at 1550 with the corrected spectrum (filled symbols) shown in **Fig. 2**. According to ref. 20, the (0-0) 1PA transition is located around 946 nm and is 1-photon forbidden due to parity selection rule<sup>21</sup>. Even though the same transition should be parity-allowed in the 2PA spectrum, the corresponding cross section is difficult to predict due to complexity of the system. Our preliminary, non-calibrated spectrum gives  $\sigma_{2\text{PA}}(1892 \text{ nm}) \sim 5 \text{ GM}$ , which is comparable to the minimum limit set by our experimental

accuracy. Interestingly, the shape of the spectrum shows no distinguishable feature at 1892 nm, which could be again due to limited accuracy of our measurement.

## Conclusions

We have studied the femtosecond 2PA cross sections and spectra of a series of linear and cyclic bytadiyne-linked zinc-porphyrin oligomers, as well as their self-assembled double-strand “ladder” and “sandwich” complexes. After backing out the resonance contribution from the measured 2-photon spectra, we find that all these systems show a strong 2-photon allowed transition in the region between the Q- and Soret bands, which we attribute to  $A_g$  type excited state. Based on the modified peak  $\sigma_{2PA}$  value, we evaluate the conjugation signature that characterizes the extent of conjugation in each structure. Comparing conjugation signature values throughout the series, we conclude that the presence of axially orientated  $\pi$ -orbitals, augmented with the structurally rigid core template and the presence of many identical porphyrin sites, provides the most efficient  $\pi$ -conjugation, as illustrated by **c-P6-T6**.

Several natural light-harvesting complexes comprise porphyrins that are arranged in ring-types geometries<sup>1,2,37,38</sup> somewhat resembling that of **c-P6-T6**. Of course, natural systems have far more complicated internal morphologies, including non-covalent binding and resonance energy transfer (predominantly) between the sub-units. Atomic force microscopy of purple photosynthetic bacteria revealed a circular architecture of the light harvesting complexes and reaction centers<sup>39</sup>. It is not clear what role does the structural rigidity play, or why did nature evolve this particular topology that seems to maximize the energy conversion. Our study shows

that qualitatively similar nanoring porphyrins with the internal template provide the most efficient conjugation among the geometries considered here.

Associated content

Supporting information

Details of UV-vis-NIR absorption measurements, denaturation titrations and fluorescence anisotropy. This material is available free of charge via the Internet at <http://pubs.acs.org>.

Author information

Corresponding author:

\*E-mail: [arebane@montana.edu](mailto:arebane@montana.edu)

\*E-mail: [harry.anderson@chem.ox.ac.uk](mailto:harry.anderson@chem.ox.ac.uk)

## **Acknowledgements**

A.R., M.D. and A.M. were supported by NIH grant R01 GM098083. A.R. acknowledges support by Estonian Ministry of Education grant IUT23-9. D.V.K., A.C. and H.L.A. thank the EPSRC and the ERC (grant 320969) for support.

## References

- (1) Milgrom, L. R. *The Colours of the Life. An Introduction to the Chemistry of Porphyrins and Related Compounds*. Oxford University Press 1997
- (2) McDermott, G.; Prince, S. M.; Freer, A. A.; Hawthornthwaite-Lawless, A. M.; Papiz, M. Z.; Cogdell, R. J.; Isaacs, N. W. Crystal Structure of an Integral Membrane Light-Harvesting Complex from Photosynthetic Bacteria. *Nature* **1994**, *374*, 517–521.
- (3) Yang, J.; Yoon, M.-C.; Yoo, H.; Kim, P.; Kim, D. Excitation Energy Transfer in Multiporphyrin Arrays with Cyclic Architectures: Towards Artificial Light-Harvesting Antenna Complexes. *Chem. Soc. Rev.* **2012**, *41*, 4808–4826.
- (4) Kim, D.; Osuka, A.; *Multiporphyrin Arrays. Fundamentals and Applications*, Pan Stanford publishing, 2012.
- (5) Drobizhev, M.; Stepanenko, Y.; Dzenis, Y.; Karotki, A.; Rebane, A.; Taylor, P. N.; Anderson, H. L. Understanding Strong Two-Photon Absorption in  $\pi$ -Conjugated Porphyrin Dimers via Double-Resonance Enhancement in a Three-Level Model. *J. Am. Chem. Soc.* **2004**, *126*, 15352-15353.
- (6) Day, P. N.; Nguyen, K. A.; Patcher, R. Calculation of One-Photon and Two-Photon Absorption Spectra of Porphyrins Using Time-Dependent Density Functional Theory. *J. Chem. Theory Comput.* **2008**, *4*, 1094-1106.
- (7) Zhu, L.; Yi, Y.; Shuai, Z.; Schmidt, K.; Zojer, E. Structure to Property Relationships for Multiphoton Absorption in Covalently Linked Porphyrin Dimers: A Correction Vector INDO/MRDCI Study. *J. Phys. Chem. A* **2007**, *11*, 8509-8518.

- (8) Drobizhev, M.; Stepanenko, Y.; Rebane, A.; Wilson, C. J.; Screen, T. E. O.; Anderson, H. L. Strong Cooperative Enhancement of Two-Photon Absorption in Double-Strand Conjugated Porphyrin Ladder Arrays. *J. Am. Chem. Soc.* **2006**, *128*, 12432-12433.
- (9) Drobizhev, M.; Stepanenko, Y.; Dzenis, Y.; Karotki, A.; Rebane, A.; Taylor, P. N.; Anderson, H. L. Extremely Strong Near-IR Two-Photon Absorption in Conjugated Porphyrin Dimers: Quantitative Description with Three-Essential-States Model. *J. Phys. Chem. B* **2005**, *109*, 7223-7236.
- (10) Peeks, M. D.; Neuhaus, P.; Anderson, H. L. Experimental and computational evaluation of the barrier to torsional rotation in a butadiyne-linked porphyrin dimer. *Phys. Chem. Chem. Phys.* **2016**
- (11) Zhang, X.-B.; Feng, J.-K.; Ren, A.-M.; Sun, C.-C. A Comparative Study of One- and Two-Photon Absorption Properties of Meso–Meso Singly, Meso- $\beta$  Doubly and Meso–Meso  $\beta$ – $\beta$ – $\beta$  Triply Linked Zn II-Porphyrin Oligomers. *J. Mol. Struct. Theochem.* **2007**, *804*, 21-29.
- (12) Varnavski, O.; Raymond, J. E.; Yoon, Z. S.; Yotsutuji, T.; Ogawa, K.; Kobuke, Y.; Goodson, T. Compact Self-Assembled Porphyrin Macrocycle: Synthesis, Cooperative Enhancement, and Ultrafast Response. *J. Phys. Chem. C* **2014**, *118*, 28474-28481.
- (13) Raymond, J. E.; Bhaskar, A.; Goodson III, Th.; Makiuchi, N.; Ogawa, K.; Kobuke, Y. Synthesis and Two-Photon Absorption Enhancement of Porphyrin Macrocycles. *J. Am. Chem. Soc.* **2008**, *130*, 17212–17213.
- (14) Easwaramoorthi, S.; Jang, S. Y.; Yoon, Z. S.; Lim, J. M.; Lee, C.-W.; Mai, C.-L.; Liu, Y.-C.; Yeh, C.-Y.; V.- Weis, J.; Wasielewski, M. R.; Kim, D. Structure–Property Relationship for

Two-Photon Absorbing Multiporphyrins: Supramolecular Assembly of Highly-Conjugated Multiporphyrinic Ladders and Prisms. *J. Phys. Chem. A* **2008**, *112*, 6563-6570.

(15) Tanihara, J.; Ogawa, K.; Kobuke, Y. Two-Photon Absorption Properties of Conjugated Supramolecular Porphyrins with Electron Donor and Acceptor. *J. Photoch. Photobio. A* **2006**, *178*, 140-149

(16) Williams-Harry, M.; Bhaskar, A.; Ramakrishna, G.; Goodson III, T.; Imamura, M.; Mawatari, A.; Nakao, K.; Enozawa, H.; Nishinaga, T.; Iyoda, M. Giant Thienylene-Acetylene-Ethylene Macrocycles with Large Two-Photon Absorption Cross Section and Semishape-Persistence. *J. Am. Chem. Soc.* **2008**, *130*, 3252–3253.

(17) Rath, H.; Sankar, J.; PrabhuRaja, V.; Chandrashekar, T. K.; Nag, A.; Goswami, D.; Core-Modified Expanded Porphyrins with Large Third-Order Nonlinear Optical Response. *J. Am. Chem. Soc.* **2005**, *127*, 11608-11609.

(18) Hunter, C. A.; Anderson, H. L. What is Cooperativity? *Angew. Chem. Int. Ed.* **2009**, *48*, 7488–7499.

(19) Ogawa, K.; Ohashi, A.; Kobuke, Y.; Kamada, K.; Ohta, K. Strong Two-Photon Absorption of Self-Assembled Butadiyne-Linked Bisporphyrin. *J. Am. Chem. Soc.* **2003**, *125*, 13356-13357.

(20) Sprafke, J. K.; Kondratuk, D. V.; Wykes, M.; Thompson, A. L.; Hoffmann, M.; Drevinskas, R.; Chen, W. H.; Yong, C. K.; Kärnbratt, J.; Bullock, J. E.; Malfois, M.; Wasielewski, M. R.; Albinsson, B.; Herz, L. M.; Zigmantas, D.; Beljonne, D.; Anderson, H. L. Belt-Shaped  $\pi$ -Systems: Relating Geometry to Electronic Structure in a Six-Porphyrin Nanoring. *J. Am. Chem. Soc.* **2011**, *133*, 17262–17273.

- (21) O'Sullivan, M. C.; Sprafke, J. K.; Kondratuk, D. V.; Rinfrey, C.; Claridge, T. D. W.; Saywell, A.; Blunt, M. O.; O'Shea, J. N.; Beton, P. H.; Malfois, M.; Anderson, H. L. Vernier Templating and Synthesis of a 12-Porphyrin Nanoring. *Nature* **2011**, *469*, 72–75.
- (22) Kondratuk, D. V.; Sprafke, J. K.; O'Sullivan, M. C.; Perdigão, L. M. A.; Saywell, A.; Malfois, M.; O'Shea, J. N.; Beton, P. H.; Thompson, A. L.; Anderson, H. L. Vernier-Templated Synthesis, Crystal Structure, and Supramolecular Chemistry of a 12-Porphyrin Nanoring. *Chem. - Eur. J.* **2014**, *20*, 12826-12834.
- (23) Taylor, P. N.; Anderson, H. L. Cooperative Self-Assembly of Double-Strand Conjugated Porphyrin Ladders. *J. Am. Chem. Soc.* **1999**, *121*, 11538-11545
- (24) Sprafke, J. K.; Odell, B.; Claridge, T. D. W.; Anderson, H. L. All-or-Nothing Cooperative Self-Assembly of an Annulene Sandwich. *Angew. Chem. Int. Ed.* **2011**, *50*, 5572–5575.
- (25) Makarov, N. S.; Drobizhev, M.; Rebane, A. Two-Photon Absorption Standards in the 550–1600 nm Excitation Wavelength Range. *Optics Express* **2008**, *16* (6), 4029.
- (26) Dubinina, G. G.; Price, R. S.; Abboud, K.A.; Wicks, G.; Wnuk, P.; Stepanenko, Y.; Drobizhev, M.; Rebane, A.; Schanze, K. S. Phenylene Vinylene Platinum(II) Acetylides with Prodigious Two-Photon Absorption. *J. Am. Chem. Soc.* **2012**, *134*, 19346–19349.
- (27) Thorne, J. R. G.; Kuebler, S. M.; Denning, R. G.; Blake, I. M.; Taylor, P. N.; Anderson, H. L. Degenerate Four-Wave Mixing Studies of Butadiyne-Linked Conjugated Porphyrin Oligomers. *Chem. Phys.* **1999**, *248*, 181-193.
- (28) Pawlicki, M.; Collins, H. A.; Denning, R. G.; Anderson, H. L. *Angew. Chem. Int. Ed.* **2009**, *48*, 3244–3266.

- (29) Hoffmann, M.; Kärnbratt, J.; Chang, M.-H.; Herz, L. M.; Albinsson, B.; Anderson, H. L. Enhanced  $\pi$  Conjugation Around a Porphyrin[6] Nanoring. *Angew. Chem. Int. Ed.* **2008**, *47*, 4993-4996.
- (30) Parkinson, P.; Kondratuk, D. V.; Menelaou, C.; Gong, J. Q.; Anderson, H. L.; Herz, L. M. Chromophores in Molecular Nanorings: When Is a Ring a Ring? *J. Phys. Chem. Lett.* **2014**, *5*, 4356-4361.
- (31) Yong, C.-K.; Parkinson, P.; Kondratuk, D. V.; Chen, W.-H.; Stannard, A.; Summerfield, A.; Sprafke, J. K.; O'Sullivan, M. C.; Beton, P. H.; Anderson, H. L.; Herz, L. M. Ultrafast Delocalization of Excitation in Synthetic Light-Harvesting Nanorings. *Chem. Sci.* **2015**, *6*, 181-189.
- (32) Chang, M.-H.; Hoffmann, M.; Anderson, H. L.; Herz, L. M. Dynamics of Excited-State Conformational Relaxation and Electronic Delocalization in Conjugated Porphyrin Oligomers. *J. Am. Chem. Soc.* **2008**, *130*, 10171-10178.
- (33) She, C.; Easwaramoorthi, S.; Kim, P.; Hiroto, S.; Hisaki, I.; Shinokubo, H.; Osuka, A.; Kim, D.; Hupp, J. T. Excess Polarizability Reveals Exciton Localization/Delocalization Controlled by Linking Positions on Porphyrin Rings in Butadiyne-Bridged Porphyrin Dimers. *J. Phys. Chem. A* **2010**, *114*, 3384-3390.
- (34) Toptygin, D. Effects of the Solvent Refractive Index and Its Dispersion on the Radiative Decay Rate and Extinction Coefficient of a Fluorescent Solute. *J. Fluoresc.* **2003**, *13*, 201-219.



- (35) Svatek, S. A.; Perdigão, L. M. A.; Stannard, A.; Wieland, M. B.; Kondratuk, D. V.; Anderson, H. L.; O'Shea, J. N.; Beton, P. H. Mechanical Stiffening of Porphyrin Nanorings through Supramolecular Columnar Stacking. *Nano Lett.* **2013**, *13*, 3391–3395.
- (36) Tait, C. E.; Neuhaus, P.; Peeks, M. D.; Anderson, H. L.; Timmel, C. R. Transient EPR reveals triplet state delocalization in a series of cyclic and linear  $\pi$ -conjugated porphyrin oligomers. *J. Am. Chem. Soc.* **2015**, *137*, 8284-8293.
- (37) Green, B. R.; Parson, W. W. Light-Harvesting Antennas in Photosynthesis. *Advances in Photosynthesis and Respiration*. Springer Science + Business Media B.V **2003**, *13*.
- (38) Hunter, C. N.; Daldal, F.; Thurnauer, M. C.; Beatty, J. T. The Purple Phototropic Bacteria. *Advances in Photosynthesis and Respiration*, Springer Science + Business Media B.V **2009**, *28*
- (39) Bahatyrova, S.; Frese, R. N.; van der Werf, K. O.; Otto, C.; Hunter, C. N.; Olsen, J. D. Flexibility and Size Heterogeneity of the LH1 Light Harvesting Complex Revealed by Atomic Force Microscopy Functional Significance for Bacterial Photosynthesis, *J. Biol. Chem.* **2004**, *279*, 21327-21333.